# Design of a ferrite rod antenna for harvesting energy from medium wave broadcast signals

*Vladimir Dyo, Tahmina Ajmal, Ben Allen, David Jazani, Ivan Ivanov*

*Centre for Wireless Research, University of Bedfordshire, Park Square, Luton LU1 3JU, UK*
*E-mail: Ben.Allen@beds.ac.uk*

Published in *The Journal of Engineering*; Received on 23rd October 2013; Accepted on 19th November 2013

**Abstract:** Radio frequency (RF) energy harvesting is an emerging technology that has the potential to eliminate the need for batteries and reduce maintenance costs of sensing applications. The antenna is one of the critical components that determines its performance and while antenna design has been well researched for the purpose of communication, the design for RF energy harvesting applications has not been widely addressed. The authors present an optimised design for such an antenna for harvesting energy from medium wave broadcast transmissions. They derive and use a model for computing the optimal antenna configuration given application requirements on output voltage and power, material costs and physical dimensions. Design requirements for powering autonomous smart meters have been considered. The proposed approach was used to obtain the antenna configuration that is able to deliver 1 mW of power to 1 kΩ load at a distance of up to 9 km, sufficient to replace batteries on low-power sensing applications. Measurements using a prototype device have been used to verify the authors simulations.

## 1 Introduction

Energy harvesting is a promising approach that may provide a solution to enabling the autonomous operation of low-power electronics and wireless sensors by extracting energy from the ambient environment. The recent emphasis on energy and the environment [1] provides a strong motivation for developing energy harvesting based operation of electronic sensors. One specific application that has received a lot of interest in recent years is smart metering. Smart meters are a constituent component of the smart grid [2] to monitor the use of utilities (water, gas and electricity) and report consumption back to the provider in near-real-time so that utility companies can provide a more accurate billing service and react to fluctuations in demand. As with current utility meters, they are likely to be located close to both commercial and residential property, with typically one per utility per property. A smart meter consists of a sensor and wireless device for reporting data, and consequently requires power to function. Energy harvesting has the advantage in making the sensors self-sustaining by harvesting energy from rich ambient sources such as sunlight, electromagnetic waves, heat gradient, wind, salinity gradients and kinetic energy. A block diagram of a generic energy harvester is shown in Fig. 1.

Here, we present the design of a radio frequency (RF) energy harvester where the antenna has been designed using mathematical optimisation. In the case of an RF energy harvester, the transducer is an antenna and the harvested energy largely depends on the optimal functioning of the antenna together with highly efficient signal conditioning circuitry which converts the RF signal to DC. This is then used to power or charge the device, such as smart meters. One of the critical components in the RF energy harvester is the antenna and while antenna design has been well researched for the purpose of communication, the design for RF energy applications presents new requirements. The challenge is to design a compact antenna that satisfies the power output requirements, fits within certain physical dimensions and cost constraints.


**Fig. 1** *Block diagram of a generic energy harvester*

In this paper, we describe the system for RF energy harvesting from medium wave (MW) broadcast signals and an optimisation approach for antenna design in this context. The key contribution of this work is the design and application of a ferrite rod antenna for RF energy harvesting applications from MW signals. The MW band is attractive for energy harvesting applications because of availability of very high-power transmitters, and a good coverage compared with higher-frequency transmitters. Our second contribution is the design optimisation for the antenna in this context. To the best of our knowledge, this is the first work that takes into account the economic dimension of the problem, and obtains the lowest cost antenna configuration given a certain set of requirements. As an example case study, we use the proposed method to optimise the design of a ferrite loop antenna for energy harvesting from a MWs transmitter. Measurement results obtained using a prototype device are used to support our findings.

In the remainder of this paper, we review RF energy harvesting technologies and their principle of operation. We then introduce our recent work on such a device that harvests energy from ambient MW signals. Finally, we summarise and conclude our paper.

## 2 RF energy harvesting

We have developed an innovative energy harvesting technology which uses a compact antenna to harvest enough energy from ambient radio waves to power electronic devices such as wireless sensor nodes and smart meters [3]. Compared with other energy harvesting techniques, harvesting energy from radio waves has the advantage in that it does not rely on light, movement or heat so long as there is sufficient coverage of the target transmission. Coverage is determined by the:

- transmitted power, frequency, transmitter antenna, receiver antenna and distance from the transmitter (i.e. Friis equation).
- physical environment between the transmitter and device, that is, path loss.
- design of the device itself, that is, antenna efficiency, circuit efficiency and power requirements.

The challenge is to identify radio signals that provide sufficient coverage, and then to design a highly efficient energy harvesting device that is compact and delivers enough power for the target application.

Intel conducted an experiment that demonstrated harvesting power from TV signals to power a digital thermometer [4]; however, the apparatus required a Yagi antenna that is far from compact. TV signals have also been investigated for powering devices in [5]. Reference [6] reports a commercial device developed by Powercast that requires a bespoke transmitter as the signal source which must be no more than approximately 3 m from the user equipment. Airenergy [7] reported a product for charging a battery using power harvested from WiFi signals. However, analysis shows that the device must be no more than a few centimetres from the WiFi access point, and even at these short distances it will take many months to fully charge a mobile phone battery. Nokia has developed an RF energy harvester that can supply 3–5 mW of power, which is not enough to power a mobile phone, but is enough to power other lower-power electronic devices such as wireless sensor network nodes and clocks [8]. Reference [9] describes an educational experiment that powers a clock from MW radio signals and requires a 20 m wire ideally strung outside. In reference [10], Sogorb *et al.* describe an experimental RF energy harvesting system operating at 1.584 MHz and use an 8 m long 'L' antenna to give 1.6 V and 8 μA. Similarly, in [11] Xie *et al.* investigated a system operating in the same frequency band, but use a 10 m horizontal wire antenna that gives 5 V and 6 μA. Sim *et al.* [12] report the design of a patch antenna for outdoor RF energy harvesting applications. Penella-López and Gasulla-Forner [13] conducted a city-wide RF survey and designed RF harvesters for operation in the DTV, GSM900, GSM1800 and third-generation frequency bands. Georgiadis *et al.* [14] describe a rectenna design method that combines electromagnetic simulation and harmonic balance analysis, and demonstrate it by designing and implementing a 2.45 GHz rectenna. Finally, Lui *et al.* [15] report a device operating at 2.45 GHz that gives 2 V at a range of 15 cm from the transmitter, which is comparable with the device in [7], but with more realistic operational expectations.

Our aim has been to seek a means of harvesting energy from ambient radio signals with a compact antenna that can enjoy better signal coverage than the devices reported in the prior art. We have targeted MW transmissions because they are often transmitted with very high power (up to 2 MW) and, compared with those at higher frequencies, propagate very well over hills and through urban conurbations. According to [16, 17], there are a large number of MW broadcast transmitters dispersed around the UK and the rest of Europe, which cover most of the major urban conurbations. All of these transmitters can be considered as high power, with RF power in excess of 150 kW and sometimes as much as 2 MW. There are even more low-power MW transmitters which we have omitted. We have identified a compact antenna and our findings show there is sufficient energy to power wireless nodes located up to 20 km from the transmitter [3]. In comparison with our earlier work described in [3, 18, 19], we

- develop and describe in detail an optimisation model used to determine the design of our antenna;
- extend our analytical model to include factors relating to rod permeability and coil self-resonant frequency (SRF); and
- measured performance for an experimental device to support our modelling and optimisation work.

## 3 Principle of operation

Our RF energy harvester uses a ferrite loop antenna chosen because it provides a compact solution at low frequencies such as MWs. It consists of $n$ turns of wire wound around a ferrite rod of coil diameter $D$ and length $\ell_{\text{coil}}$, and which has an effective permeability of $\mu_{\text{eff}}$ (Fig. 2*a*). The equivalent circuit of the energy harvester consists of a ferromagnetic loop antenna tuned with a capacitance $C$, and a load connected across the capacitor (Fig. 2*b*). The open-circuit voltage across the capacitor ($V_{\text{c}}$) at resonance is [20]

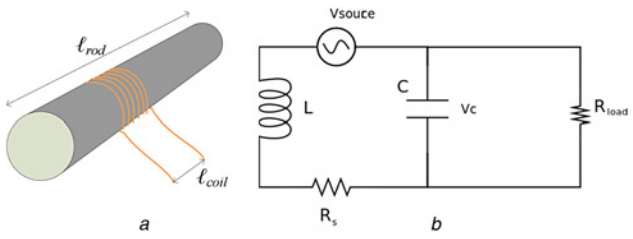


**Fig. 2** *Principle of operation*
*a* Schematic of a rod antenna
*b* Equivalent circuit of a rod antenna with a connected load

$$V_{\text{c}} = I_{\text{c}} Z_{\text{c}} = \frac{V_{\text{source}}}{R_{\text{s}}} \frac{1}{\omega C} = Q V_{\text{source}} \tag{1}$$

where $I_{\text{c}}$ and $Z_{\text{c}}$ are the currents through the capacity and capacitor impedance, respectively, $Q$ is the quality factor for the circuit at resonance, defined as

$$Q = \frac{1}{R_{\text{s}} \omega C} = \frac{\omega L}{R_{\text{s}}} \tag{2}$$

The induced voltage, $V_{\text{source}}$, for a ferromagnetic loop antenna assuming the incident electric field strength $E$ is given by [20, 21]

$$V_{\text{source}} = \frac{2\pi}{\lambda} E \frac{\pi D^2}{4} n \cos\theta \tag{3}$$

By substituting (2) and (3) into (1) we obtain

$$V_{\text{C}} = Q V_{\text{source}} = Q \frac{2\pi}{\lambda} E \frac{\pi D^2}{4} n \cos\theta \tag{4}$$

$Q$ is the unloaded coil quality factor and $L$ is the coil inductance. Here, $f$ is the carrier frequency, $\lambda$ is the wavelength, $R_{\text{s}}$ is the antenna coil series resistance and $\theta$ is the alignment angle with electric field. The antenna terminals are connected to the RF-DC convertor circuitry and matched to maximise the available voltage.

### 3.1 Antenna inductance and effective permeability

The antenna inductance is given as [20]

$$L = \frac{n^2 A \mu_{\text{eff}} \mu_o}{\ell_{\text{coil}}} \tag{5}$$

$A$ is the cross-sectional area of the coil, $\mu_{\text{eff}}$ is the effective permeability of ferrite rod that has relative permeability $\mu_{\text{r}}$ and $\mu_0$ is an absolute permeability. The effective permeability of core $\mu_{\text{eff}}$ depends on two factors

(1) geometry and dimensions of the ferrite rod. For cylindrically shaped rods, the permeability of the rod is given as

$$\mu_{\text{rod}} = \frac{\mu_{\text{r}}}{1 + (\mu_{\text{r}} + 1)(D/\ell_{\text{rod}})^2 \left(\ln(\ell_{\text{rod}}/D)\{0.5 + 0.7[1 - \exp(-\mu_{\text{r}} \times 10^{-3})]\}\right)} \tag{6}$$

According to this expression, the permeability of the rod increases with $\ell_{\text{rod}}/D$ ratio and peaks at $\ell_{\text{rod}}/D = 20$ [21] irrespective of the rod diameter. Expression (8) is valid for rod antennas with $\ell_{\text{rod}}/D$



*J Eng 2013*
doi: 10.1049/joe.2013.0126

ratio of between 2 and 100. Various modifications are possible in the design of the antenna to improve the effective permeability. These include changing the cylindrical shape of the rod to a hyperboloid or dumbbell [21]. In this work, we consider a ferrite rod antenna that is cylindrical in shape, with the coil covering the entire length of the rod.

(2) The placement of the coil along the ferrite rod. The explanation of the physical phenomena is beyond the scope of this paper, but we provide a short summary from [12]. As the ferrite rod is not a perfect director of flux, some flux lines exit the rod closer from the sides. As a result, these leakage flux lines will not pass through all the turns of the coil, thus reducing the effective permeability of the rod. Consequently, shorter coils concentrated in the centre of the rod result in higher-effective rod permeability, whereas coils spanning an entire length of the rod will have a lower-effective rod permeability. To describe this behaviour, for a ferrite rod length $\ell_{\text{rod}}$ and coil length $\ell_{\text{coil}}$, the effective permeability is adjusted as [22, 23]

$$\mu_{\text{eff}} = \mu_{\text{rod}} \sqrt[3]{\frac{\ell_{\text{rod}}}{\ell_{\text{coil}}}} \tag{7}$$

### 3.2 *Self-resonant frequency*

Self-resonant frequency, $f_{\text{SRF}}$, determines the upper limit of the operating frequency for the coil as it is the highest frequency for which the coil is inductive [24]. The self-resonance frequency depends on its inductance $L$ and parasitic capacitance $C_{\text{paras}}$, and is therefore a function of its physical dimensions

$$f_{\text{SRF}} = \frac{1}{2\pi\sqrt{\text{LC}_{\text{paras}}}} \tag{8}$$

Thus, for a given coil inductance and target SRF, the maximum value of capacitance must be kept below

$$C_{\max} = \frac{1}{4\pi^2 f_{\text{SRF}}^2 L} \tag{9}$$

For single layer coils, an approximate value of coil parasitic capacitance can be computed using the model described in [25]

$$C_{\text{paras}} = 1.366 C_{tt} \tag{10}$$

$$C_{tt} = \varepsilon_0 l_{\text{t}} \left[ \frac{\varepsilon_{\text{r}} \theta^*}{\ln(d_0/d_{\text{c}})} + \cot\left(\frac{\theta^*}{2}\right) - \cot\left(\frac{\pi}{12}\right) \right] \tag{11}$$

$$\theta^* = \arccos\left(1 - \frac{\ln(d_0/d_{\text{c}})}{\varepsilon_{\text{r}}}\right) \tag{12}$$

where $C_{tt}$ is the parasitic capacitance between adjacent turns of the wire, $d_0$ is the outer diameter of the wire including an insulator, $d_{\text{c}}$ is the diameter of the wire core (conductor), $l_{\text{t}}$ is the length of a single turn of wire and $\varepsilon_0$ is absolute permittivity. Thus, the coil parasitic capacitance is a function of coil diameter, insulator thickness and a diameter of the conducting part of the wire.

The values of self-capacitance predicted by the model have been compared with the measured values and in an illustrative example were shown to be within 17.2% [25]. We have constructed a range of coils of different configurations shown in chronological order in Fig. 3.

## 4 RF energy from MW transmitters

We assume the RF energy harvester is located at a distance $d$ from the MW transmitter. For operation in the MW band, $E$ is computed using the model described in [20] as follows. For an antenna with a figure-of-merit (FM) and transmitted power, $P_{\text{t}}$, the electric field, $E$, at distance $d$ can be given as

$$E = \text{FM}\frac{\sqrt{P_{\text{t}}}}{d} A \tag{13}$$

Here, $A$ is the attenuation factor and depends on the distance from the transmitter ($d$), carrier frequency ($f$) and the earths' conductivity ($\sigma$) and relative permittivity of the ground path ($\varepsilon_{\text{r}}$). This is given as

$$A = \frac{2 + 0.3p}{2 + p + 0.6p^2} - (\sin b^\circ)\sqrt{\frac{1}{2}p}\exp(-5p/8) \tag{14}$$

where the auxiliary parameters, $p$ and $b^\circ$ are defined as $p = \left(0.582df^2 \cos b^\circ\right)/\sigma$

$$b^\circ = \tan^{-1}\left(\frac{(\varepsilon_{\text{r}} - 1)f}{18\sigma}\right) \tag{15}$$

The FM of an antenna, for a vertical monopole is given as

$$\text{FM} = \frac{60\sqrt{1000}(1 - \cos \beta h)}{\sqrt{R_{\text{L}}}} \tag{16}$$

where $R_{\text{L}}$ and $h$ are loop resistance and the height of the monopole, respectively, and $\beta = 2\pi/\lambda$ is a phase change coefficient. Equations (1)–(5) present us with an analytical means for determining the RF power harvesting performance when coupled with transmitter and signal propagation parameters. As an illustration, Fig. 4*a* shows the energy available from a MW transmitter that emits 150 kW of RF power at 1 MHz and harvested by an ideal ferrite rod antenna. We assume $\sigma = 1$ mS and $\varepsilon_{\text{r}} = 3$ [23], an antenna constructed of 200 turns of silk-covered 0.07 mm diameter litz wire wound around an insulator tube with a diameter of 10 mm and length 200 mm. The insulator is placed around a ferrite rod with a relative permeability of 300, and hence an effective permeability of 10. With the device aligned to maximise the resulting induced voltage, this yields an alternating voltage reducing from 2.6 to 0.3 mV across the open-circuit terminals of the windings as the distance from transmitter increases to 100 km. Fig. 4*a* shows how the power into the 1 kΩ load diminishes from 3.5 mW down to 55 pW as distance increases. Fig. 4*b* shows the dependency of generated voltage on $\ell_{\text{rod}}/D$ ratio for different core diameters, $D$. Device

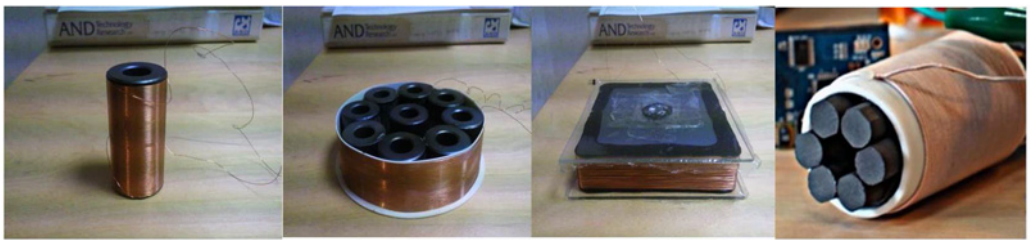

**Fig. 3** *Early antenna prototypes*

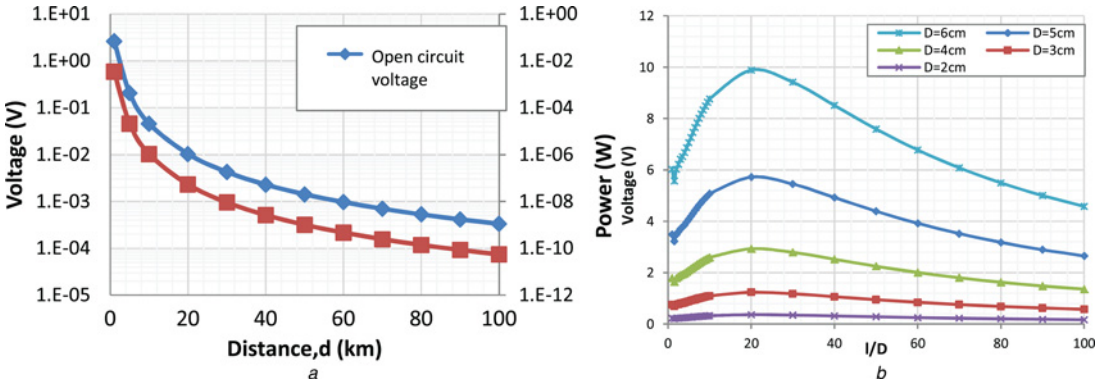


**Fig. 4** *RF energy from MW transmitters*
*a* Open-circuit voltage across the antenna terminals against distance from the transmitter. Load power against distance from the transmitter
*b* Open-circuit voltage as a function of coil length-to-diameter ratio ($l_{rod}/D$)

performance depends on many different factors, including antenna geometry, dimensions, number of turns and the type of wire. Simulations have shown that the effective permeability of the antenna is the dominant factor in determining the optimal configuration. A peak in open-circuit voltage occurs at $\ell_{rod}/D = 20$ (for all values of $D$), which corresponds to configurations with maximum values of effective rod permeability.

In the next section, we consider the optimisation of antenna parameters, where we confirm these findings, and impose some more realistic constraints. An optimisation takes into account SRF, effective permeability and wire characteristics.

## 5 Antenna design optimisation

### 5.1 Optimising antenna design

Design requirements may be achieved through many different combinations of antenna parameters. For example, the same output voltage can be produced by a short and wide coil with high number of turns, or long and thin coil, which benefits from a higher-effective permeability, and thus fewer turns. Each configuration will have a different cost in terms of materials. The goal of the optimisation is to minimise the antenna cost function while providing a target output voltage $V_{target}$, target output power $P_{target}$ and satisfying constraints on physical dimensions ($D_{min}$, $D_{max}$, $l_{min}$ and $l_{max}$), SRF $f_{SRF}$ and $Q$ factor. The optimisation procedure searches through the parameter space for the configuration that has the lowest cost while satisfying the design constraints. We define the objective function $F(l_{coil}, D, s)$, as a function of coil length ($l_{coil}$), coil diameter ($D$) and wire length ($s$). The optimisation problem is then formulated as follows

$$\min F\left(l_{coil},\ D,\ s\right) = \frac{\pi D^2}{4} l_{coil} P_f + s P_w + l_{coil} P_l \tag{17}$$

$$\text{s.t. } P_{load} \geq P_{target}, \quad V_{loaded} \geq V_{target}, \quad Q \leq Q_{max} \tag{18}$$

$$\begin{aligned} &D_{min} < D < D_{max} \\ &l_{min} < l_{coil} < l_{max} \\ &2D < l_{coil} < 100D \end{aligned} \tag{19}$$

$$f_{SRF} < F_{SRF\_MAX} \tag{20}$$

The terms in (17) represent the ferrite and wire costs, coil length and diameter, respectively. $P_f$ and $P_w$ are the costs of ferrite and wire per unit volume and per unit length, respectively. $P_l$ and $P_D$ are the penalty coefficients for length and diameter of the antenna to tune the optimisation process. If the antenna needs to be fitted within an enclosure of a certain size, for example, increasing the penalty factor for coil length $P_l$ will drive the optimisation towards configurations with shorter coils. For RF energy harvesting applications, one design objective is also to control the bandwidth of the antenna, for example, to tune to a certain narrow band signal. This can be done by controlling the $Q_{max}$ constraint, which also impacts several other design parameters of the coil and rod. The coefficients are set to zero if there are no specific requirements for antenna dimensions.

The proposed optimisation approach takes into account key design factors including the effective permeability of the ferrite rod, parasitic capacitance and the SRF. The effective permeability of the rod is computed using (6) given ferrite rod dimensions ($l_{coil} \times D$). Here, the coil and rod dimensions are assumed to be the same; modifying the approach for different coil and rod dimensions is straightforward. The SRF for the coil, $f_{SRF}$, is given by (8) and a model for parasitic capacitance of single layer coils given by (10–12).

To reduce skin and proximity effects present at RF frequencies, a litz wire, which consists of a number of fine electrically isolated strands, is assumed to be used in the coil construction. We compute the resistance of a coil comprising litz wire, $R_s$ by dividing the total resistance of wire by the number of strands

$$R_s = \frac{R_{total}}{N_{str}} \tag{21}$$

where $\rho$ and $d$ are the relative resistivity of copper and the diameter of a strand, respectively. The variable $s$ represents the total length of all strands. The number of strands, $N_{str}$, in a litz wire is provided as an input parameter and will be discussed in more detail in Section 6. The number of turns of wire, $n$, needed to compute coil inductance (5), is expressed through a total wire length, $s$ and coil diameter, $D$

$$n = \frac{s}{\pi D N_{str}} \tag{22}$$

The open-circuit voltage generated by the antenna is described by (1). The loaded voltage will depend on the value of $Z_{load}$ and is computed using the voltage divider rule [23]

$$V_{loaded} = \frac{V_{out} Z_{load}}{Z_{coil} + Z_{load}} \tag{23}$$

The power delivered to the load is computed as

$$P_{load} = \frac{V_{out}^2 Z_{load}}{\left(Z_{coil} + Z_{load}\right)^2} \eta \tag{24}$$

where $Z_{coil} = R_{coil} + j\omega L$ is coil impedance. $Z_{load}$ is the input impedance of the RF-DC convertor circuitry and is provided as an input parameter. Delivering maximum power to the load requires conjugate matching of the load, and will be discussed in more detail in Section 6. $\eta$ is the efficiency of the RF-DC conversion circuit and is assumed for this example to be 50% as reported in reference [13]. In practice, the value of $\eta$ is a function of the incident voltage.

## 6 Design case study

We use the above method to find an optimal configuration for a ferrite rod antenna to harvest energy from a BBC Radio 5 transmitter located in Brooksman Park, UK, at a range of distances from 1 to 15 km. The transmitter emits 150 kW of RF power at 909 kHz. The energy harvester is required to deliver 1 mW of power to a 1 kΩ resistor, have 50% power efficiency and have a 1 V voltage across the load. These parameters are indicative of the power requirements for smart meters. The load capacitance is assumed to be matched to the energy harvester. The ferrite rod and coil dimensions are assumed to be equal, that is, the coil spans the entire length of the ferrite rod, and the insulator tube thickness around the rod is negligible. The energy harvester is assumed to drive a 1 kΩ resistor, have 50% power efficiency and require a 0.3 V start-up voltage.

Table 2 contains the rest of the design parameters. The optimisation model was implemented and simulated using the sequential quadratic programming algorithm in the MATLAB R2012 optimisation toolbox. The objective function, $\boldsymbol{f}$, is convex as its Hessian matrix, $\boldsymbol{H}$, is positive semi-definite [26]. The Hessian $\boldsymbol{H}(\boldsymbol{f})$ of the objective function (17) and the eigenvalues, $\lambda$, of the Hessian are given below (derivation is in the appendix)

$$\boldsymbol{H}(\boldsymbol{f}) = \begin{matrix} 0 & \pi D/2 & 0 \\ \pi D/2 & \pi l_{coil}/2 & 0 \\ 0 & 0 & 0 \end{matrix} \qquad 0$$

$$\boldsymbol{\lambda} = \frac{\pi l_{coil}}{4} - \frac{\pi}{2}\left(\frac{l_{coil}^2}{4} + D^2\right)^{1/2}$$

$$\frac{\pi l_{coil}}{4} + \frac{\pi}{2}\left(\frac{l_{coil}^2}{2} + D^2\right)^{1/2}$$

The eigenvalues $\lambda$ of the Hessian matrix are non-negative for $l_{coil} < 1$ m, so the matrix is positive semi-definite [26]. For convex functions, a local minimiser is also a global minimiser [27]. The constraint function results in a fourth degree polynomial, for which a convexity test is complicated. For this reason to obtain a global minimum, we used a heuristic approach together with a number of start points, with one of the start points leading to a global minimum. The convergence of the solutions was then checked by plotting the best function value and the number of iterations (Fig. 5). Fig. 5 shows the best function value achieved by each local solver, and the total number of function evaluations for one set of design parameters. The start points were randomly generated within the problem constraints (Table 1) and solved using local solvers.

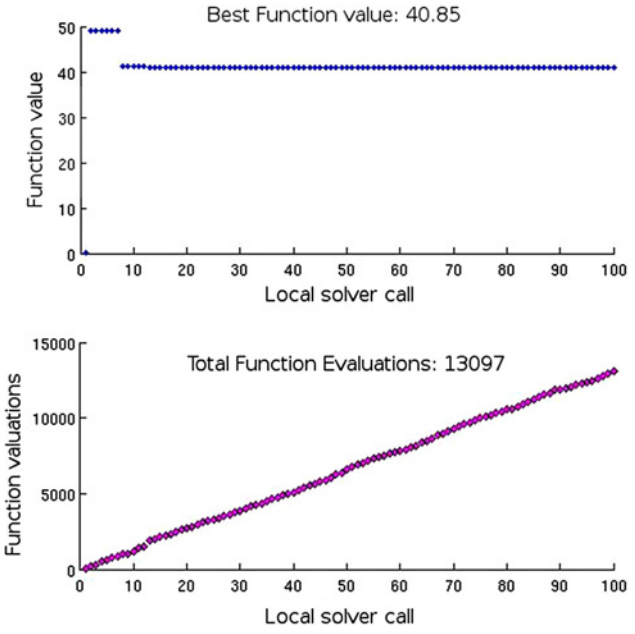


**Fig. 5** *Best objective function value and number of evaluations against local solver call*

Table 2 and Fig. 6 show the optimum antenna configuration and cost as a function of distance from the transmitter. Each point on the graph in Fig. 6 represents the cost of an optimal antenna configuration for each distance. Note that for each distance, an optimum antenna design is determined. Consequently, as the signal strength diminishes with distance, more turns are required in order to maintain performance. As a result, the SRF reduces, as can be seen by the curve. For distances larger than 8.5 km, the SRF falls below the transmitter frequency thus making performance impossible to maintain in practice.

Table 2 shows that the optimal rod dimensions are the same for all transmitter distances (i.e. $0.20 \times 0.01$ m$^2$), and the antenna configurations differ in the length of wire and the number of turns. The optimisation process selects the smallest possible rod dimension that provides the maximum effective permeability of the rod (which reaches its maximum at $\ell_{rod}/D \simeq 20$, see Fig. 4*b*). The required target voltage is achieved through varying the number of turns and the length of wire. This behaviour is also consistent with the model. By substituting (21), (22) into (1), we obtain (25), which suggests that for a given *D*/*l* ratio, the coil open-circuit voltage is a function of the length of wire

$$E = \frac{\pi f \mathrm{E}}{4\lambda\rho}\left(\frac{D}{l_{coil}}\right)s^2 \tag{25}$$

The rod dimensions are sensitive to ferrite cost and coil $Q$ factor. Consequently, the cost of ferrite yields antennas with smaller (shorter) rods with more wire (more turns). The constraint on the

**Table 1** Design parameters

| Design parameter, units | Values | Design parameter, units | Values | Design parameter, units | Values |
|---|---|---|---|---|---|
| $V_{out}$, $V$ | 1.0 | $P_w$, £/$m$ | 0.08 | transmitter power | 150 kW |
| $\mu_r$, $H$ m$^{-1}$ | 300 | $P_f$, £/m$^3$ | 412 | distance from the transmitter | 1.15 km |
| $d$, $m$ | $0.07 \times 10^{-3}$ | $\rho$, Ω $m$ | $1.68 \times 10^{-8}$ | load resistance | 1 kΩ |
| $D_{min}$, $l_{min}$, $m$ | 0.01 | $D_{max}$, $l_{max}$, $m$ | 0.6 | converter efficiency | 50% |
| $d_0$, $m$ | $5.55 \times 10^{-4}$ | $d_c$, $m$ | $6 \times 10^{-4}$ | start-up voltage | 0.3 V |
| $\varepsilon_0$, $F/m$ | $8.85 \times 10^{-12}$ | $\varepsilon_r$ | 3.5 | | |

**Table 2** Optimal antenna configurations for distances 1–15 km

| Distances, km | *l*, *m* | *D*, *m* | *s*, *m* | *n* | *L*, *H* | Distances, km | *l*, *m* | *D*, *m* | *s*, *m* | *n* | *L*, *H* |
|---|---|---|---|---|---|---|---|---|---|---|---|
| 1 | 0.2 | 0.01 | 67 | 48 | $1.325 \times 10^{-4}$ | 9 | 0.2 | 0.01 | 457 | 323 | $6.100 \times 10^{-3}$ |
| 2 | 0.2 | 0.01 | 110 | 78 | $3.556 \times 10^{-4}$ | 10 | 0.2 | 0.01 | 511 | 361 | $7.613 \times 10^{-3}$ |
| 3 | 0.2 | 0.01 | 155 | 110 | $7.010 \times 10^{-4}$ | 11 | 0.2 | 0.01 | 565 | 399 | $9.314 \times 10^{-3}$ |
| 4 | 0.2 | 0.01 | 202 | 143 | $1.190 \times 10^{-3}$ | 12 | 0.2 | 0.01 | 619 | 438 | $1.121 \times 10^{-2}$ |
| 5 | 0.2 | 0.01 | 251 | 177 | $1.835 \times 10^{-3}$ | 13 | 0.2 | 0.01 | 675 | 477 | $1.330 \times 10^{-2}$ |
| 6 | 0.2 | 0.01 | 301 | 213 | $2.643 \times 10^{-3}$ | 14 | 0.2 | 0.01 | 731 | 517 | $1.560 \times 10^{-2}$ |
| 7 | 0.2 | 0.01 | 352 | 249 | $3.620 \times 10^{-3}$ | 15 | 0.2 | 0.01 | 787 | 557 | $1.811 \times 10^{-2}$ |
| 8 | 0.2 | 0.01 | 404 | 286 | $4.771 \times 10^{-3}$ | | | | | | |

maximum value of $Q$ factor drives the optimisation towards solutions with lower coil inductance and consequently requires longer wire to maintain the same level of output voltage. The inductance is reduced by increasing the diameter of the coil. Note that inductance can also be reduced by shortening the rod while keeping the original diameter; yet, the results indicate that increasing the diameter results in a lower cost than shortening the rod.

### 6.1 *Self-resonant frequency*

Fig 7 shows the SRF of antenna configurations from the results obtained in the previous exercise (Table 3). At larger distances, producing the required level of voltage and power requires higher inductance. The problem is that the higher inductance reduces the SRF, which becomes a major limiting factor. Increasing the operating range of the energy harvesting device requires reducing either inductance or parasitic capacitance of a coil.

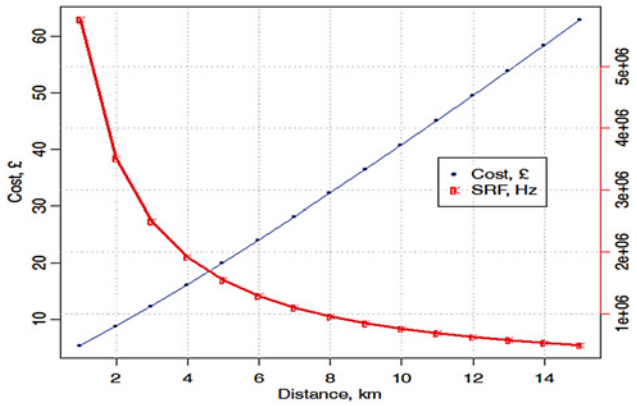


**Fig. 6** *Antenna cost and performance against distance, 45 strands*

### 6.2 *Number of strands in litz wire*

Litz wire is used in RF applications to reduce skin and proximity effects associated with high-frequency currents. It consists of a number of strands, and has a lower resistance to high-frequency current. An interesting design question is whether to use shorter wire with more strands or longer wire with fewer strands. The first option would result in fewer turns, but lower internal resistance, lower losses within the coil and therefore higher efficiency. On the other hand, the second option would result in more turns, and consequently higher voltage and output power.

To investigate the impact of number of litz wire strands on antenna performance, we have repeated the experiment with the same transmitter, but for different litz wire configurations. Figs. 7*a* and *b* show the antenna SRF performance and cost for a litz wire with 15 and 60 strands. They show that the configurations with lower number of strands result in lower cost, but also lower SRF. It can also be observed that reducing the number of strands increases coil inductance. Intuitively, reducing the number of strands result in higher coil resistance, so a higher number of turns (and therefore inductance) is required to provide the target output power and voltage. With reference to Fig. 7*a*, the maximum operating distance as a result of the antenna SRF when using litz wire of 15 and 60 strands is 4.9 and 9 km, respectively. Therefore, increasing the number of strands can also be used as a

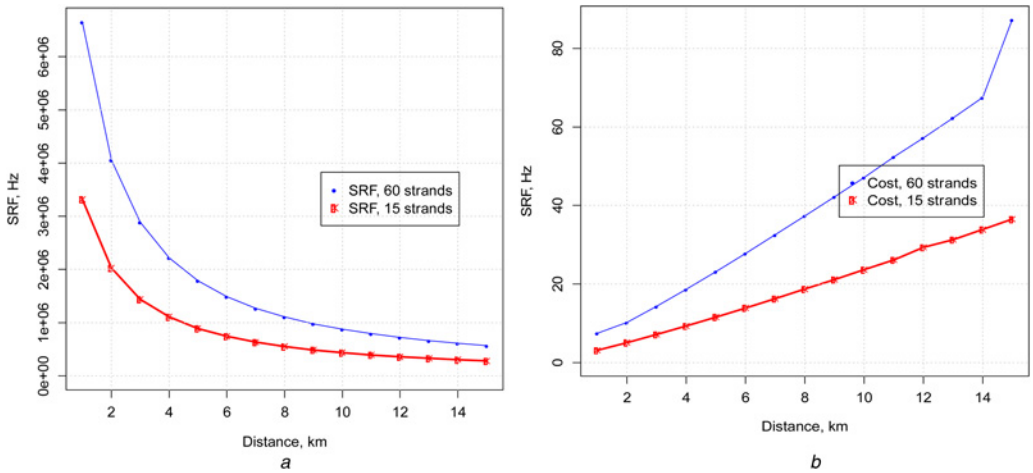


**Fig. 7** *Antenna cost and performance for different wire configurations*
*a* SRF against distance, 15 and 60 strands
*b* Cost against distance, 15 and 60 strands



*J Eng 2013*
doi: 10.1049/joe.2013.0126

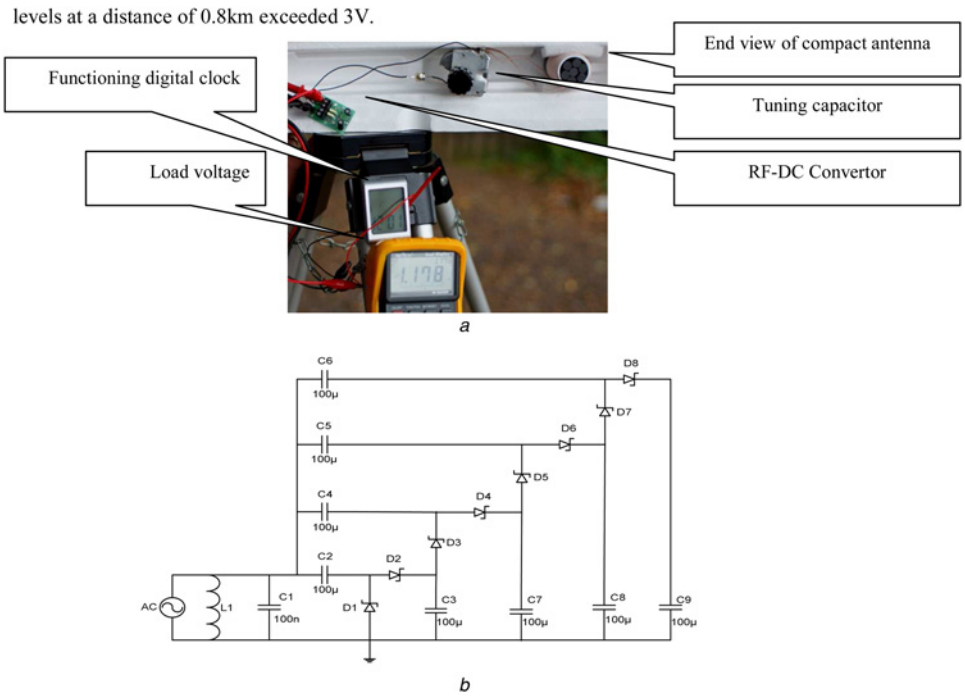


**Fig. 8** *Experimental RF energy harvester*
*a* Powering an LCD clock from RF energy
*b* RF-DC conversion circuit

way to moderately increase the operating range of the antenna. It should be possible to add $N_{str}$, the number of strands, to the list of design variables, and obtain it automatically through an optimisation process. The authors have experimented with this and obtained positive results, to be reported later.

This case study has demonstrated how the proposed optimisation method can be used to explore various design options of the antenna, as well as to identify some key limitations regarding the cost, the SRF and the operating range of RF energy harvesting devices. It has enabled us to obtain the optimal design of an RF energy harvester as given in Table 3.

## 7 RF-DC conversion circuit

We have constructed a device able to power a liquid crystal display (LCD) digital clock from 909 kHz MW broadcast signals, at a distance from 2.4 km from the Brookmans Park transmitter, as shown in Fig. 8*a*. The clock requires 1 V DC to operate, and draws 3 µA. The DC is derived from the RF signal by means of a rectifier-multiplier circuit [13] and is shown in Fig. 8*b*. Schottky diodes have been selected because of their lower switch-on voltage compared with silicon diodes. We have also conducted a set of experiments to measure the amount of power available from the Brookmans Park transmitter at a range of distances. The measurements showed RF voltage levels 3 mV–3 V across 10 kΩ load and power levels of −3 to 34 dBm for distances from 2.4 to 14.4 km. The voltage levels at a distance of 0.8 **k**m exceeded 3 V.

## 8 Discussion

Wireless sensor networks require energy for sensing, processing and transmitting data to a remote data collector. Smart meters may also require energy for displaying the information on an LCD screen, updating tariffs and actuating a shutoff valve (e.g. in case of abnormal gas or water pressure, accident, or an earthquake). Communication cost dominates the energy budget of a typical sensing application and depends on data generation interval, number of hops and network configuration. However, in low data-rate delay tolerant applications, such as smart metering, operation at ultra-low duty cycles of 0.1–0.2% is possible, which for a typical sensor node [28] translates into 78–138 µW of power. Sensor power requirements range from a few microwatts for temperature and humidity sensors to hundreds of microwatts for flow meters used in gas, water and heat sensors. When describing typical battery requirements for a metering function, Dittrich [29] specifies 5.12 mW as the average power consumption for an ultrasound gas meter.

Our proposed system provides at least 1 mW of power at a distance of 9 km from the transmitter; sufficient to operate a wireless sensor node such as Tmote Sky [28] at 1.7% duty-cycle. The proposed system can also be used in smart meters or any other electric appliances that are powered from the mains, but require a backup source of power for keeping real-time clocks or other critical functionality during power outages. More power becomes available by positioning the device closer to the transmitter.

## 9 Conclusions

In this paper, we have presented a system for RF energy harvesting from MW transmitters and proposed a design optimisation approach. The method was used to generate optimal antenna configurations for distances of up to 15 km. The analysis shows that the proposed design is able to deliver 1 mW of power to 1 kΩ load at a distance of up to 9 km from a 150 kW transmitter. The maximum power for a certain distance is fundamentally limited by the self-resonance frequency of antenna. The latter can be reduced by increasing the number of strands in the litz wire to reduce the self-capacitance of the coil. This however increases the cost of the antenna as shown by the analysis. The costs can be reduced by applying economies of scale because of the market potential of the devices. The proposed design has great potential for powering smart meters from MW transmitters and to eliminate the need for replacing or recharging the batteries, significantly reducing the maintenance costs. Potential future work includes further experimental validation of the approach and introducing additional factors into the design process to enable a direct comparison between experimental and modelled performance. These facts are: conversion efficiency $\eta$ and rod topology.

## 10 References


[1] 'The green deal: a summary of the governments proposals', 2012. Available at http://www.decc.gov.uk

[2] Santacana E., Rackliffe G., Tang L., Xiaming F.: 'Getting smart', *IEEE Power Energy Mag.*, 2012, **8**, (2), pp. 41–48

[3] Ajmal T., Jazani D., Allen B.: 'Design of a compact RF energy harvester for wireless sensor networks'. IET Conf. Wireless Sensor Systems (WSS 2012), London, UK, June 18–19 2012

[4] Sample A., Smith J.R.: 'Experimental results with two wireless power transfer systems'. IEEE Radio and Wireless Symp., 18–22 January, 2009

[5] Nishimoto H., Kawahara Y., Asami T.: 'Prototype implementation of wireless sensor network using TV broadcast RF energy harvesting'. Proc. 12th ACM Int. Conf. Ubiquitous computing, 2010, pp. 373–374

[6] Powercast RF Energy Harvesting and Wireless Power for Low-Power Application [Online]. Available at http://www.powercastco.com/PDF/powercast-overview.pdf, last accessed 31 January 2013

[7] Analysis of RCA Airnergy WiFi Energy Harvester [Online]. Available at http://www.rfwirelesssensors.com/2010/01/analysis-of-rca-airnergy-wifi-energy-harvester/, last accessed 31 January 2013

[8] NOKIA working on energy-harvesting handset: EE Times New [Online]. Available at http://www.eetimes.com/electronics-news/4195530/Nokia-working-on-energy-harvesting-handset, last accessed 31 January 2013

[9] Mindset Solid Core Wire specifications [Online]: Available at http://www.mindsetsonline.co.uk/product_info.php?products_id=1009711, last accessed 31 January 2013

[10] Sogorb T., Llario J.V., Pelegri J., Lajara R., Alberola J.: 'Studying the feasibility of energy harvesting from broadcast RF station for WSN'. IEEE Int. Instrumentation and Measurement Conf., Vancouver, Canada, 2008

[11] Xie K., Liu Y.-M., Zhang H.-L., Fu L.-Z.: 'Harvest the ambient AM broadcast radio energy for wireless sensors', *J. Electromagn. Waves Appl.*, 2011, **25**, pp. 2054–2065

[12] Sim Z., Shuttleworth R., Alexander M., Grieve B.: 'Compact patch antenna design for outdoor RF energy harvesting in wireless sensor networks', *Prog. Electromagn. Res.*, 2010, **105**, pp. 273–294

[13] Penella-López M.P., Gasulla-Forner M.: 'Powering autonomous sensors' (Springer, 2011), Chapter 6, ISBN 9789400715721

[14] Georgiadis A., Andia G., Collado A.: 'Rectenna design and optimization using reciprocity theory and harmonic balance analysis for electromagnetic (EM) energy harvesting', *IEEE Antennas Wirel. Propag. Lett.*, 2010, **9**, pp. 444–446

[15] Lui K.W., Vilches A., Toumazou C.: 'Ultra-efficient microwave harvesting system for battery-less micropower microcontroller platform', *IET Microw. Antennas Propag.*, 2011, **5**, (7), pp. 811–817

[16] Medium Wave Radio Transmitters [Online]: Available at http://www.mediumwaveradio.com/uk.php, last accessed 31 January 2013

[17] Available at http://www.mediumwave.de, last accessed 31 January 2013

[18] Ajmal T., Dyo V., Allen B., Ivanov I.: 'Design and optimisation of a compact RF energy harvesting device for smart applications', *IET Electron. Lett.*, DOI: 10.1049/el.2013.3434

[19] Allen B., Ajmal T., Dyo V., Jazani D.: 'Harvesting energy from ambient radio signals: a load of hot air?'. Keynote paper, Loughborough Antennas & Propagation Conf., Loughborough, November 2012

[20] Griffiths J.: 'Radio wave propagation and antennas – an introduction' (Prentice-Hall, 1987), pp. 33–48 and pp. 59–60

[21] Lo Y.T., Lee S.W.: 'Antenna handbook: antenna theory' (Springer, 1993, 1st edn.)

[22] 'The ARRL antenna book' (pub. ARRL, 2007, 21st edn.), Ch 5

[23] Dennison M., Fielding J.: 'RSGB radio communication handbook' (Radio Society of Great Britain, 2012, 11th edn.)

[24] Glisson T.H.: 'Introduction to circuit analysis and design' (Springer, 2011, edn.), ISBN-13: 978-9048194421

[25] Massarini A., Kazimierczuk M.K.: 'Self-capacitance of inductors', *IEEE Trans. Power Electron.*, 1997, **12**, (4), pp. 671–676

[26] Ganguly S., Mukherjee M.N.: 'A treatise on basic algebra' (Academic Publishers, 2012)

[27] Fletcher R.: 'Practical methods of optimization'. (2006, Wiley, 2nd edn.)

[28] Tmote Sky datasheet. Available at http://www.sentilla.com/pdf/eol/tmote-sky-datasheet.pdf, last accessed 31 January 2013

[29] Dittrich T.: 'Battery concepts for smart utility meters – the requirements and providing their suitability'. Tadiran Batteries GmbH


## 11 Appendix

Derivation of Hessian Matrix, $\boldsymbol{H}$. The matrix is obtained by taking second-order partial derivatives of the objective function

$$\boldsymbol{H}(f) = \begin{matrix} \frac{\partial^2 f}{\partial l^2} & \frac{\partial^2 f}{\partial l \partial D} & \frac{\partial^2 f}{\partial l \partial s} \\ \frac{\partial^2 f}{\partial D \partial l} & \frac{\partial^2 f}{\partial D^2} & \frac{\partial^2 f}{\partial D \partial s} \\ \frac{\partial^2 f}{\partial s \partial l} & \frac{\partial^2 f}{\partial s \partial D} & \frac{\partial^2 f}{\partial s^2} \end{matrix}$$

The partial derivatives are shown below

$$\frac{\partial^2 f}{\partial l^2} = 0, \quad \frac{\partial^2 f}{\partial l \partial D} = \pi D/2, \quad \frac{\partial^2 f}{\partial l \partial s} = 0$$

$$\frac{\partial^2 f}{\partial D \partial l} = \frac{\pi D}{2}, \quad \frac{\partial^2 f}{\partial D^2} = \frac{\pi l_{\text{coil}}}{2}, \quad \frac{\partial^2 f}{\partial D \partial s} = 0$$

$$\frac{\partial^2 f}{\partial s \partial l} = 0, \quad \frac{\partial^2 f}{\partial s \partial D} = 0, \quad \frac{\partial^2 f}{\partial s^2} = 0$$